THE ASTROPHYSICAL JOURNAL, 410:179–187, 1993 June 10

EXTENDED CO(7 → 6) EMISSION FROM WARM GAS IN ORION

J. E. HOWE,[1,2] D. T. JAFFE,[1] E. N. GROSSMAN,[1,3] W. F. WALL,[1,4] J. G. MANGUM,[1] AND G. J. STACEY[5]

Received 1992 October 2; accepted 1992 December 14

ABSTRACT

We mapped the quiescent emission from the 807 GHz $J = 7 \rightarrow 6$ transition of CO in Orion along a strip in R.A. extending from 0.7 pc west to 1.2 pc east of θ^1C Orionis. The lines arise in warm gas with temperatures greater than 40 K. The line brightness temperature is greater than 160 K in the direction of θ^1C, more than twice the dust temperature, and still exceeds 35 K more than a parsec east of θ^1C. The lines are narrow, with a maximum velocity width of 7 km s^{-1} near θ^1C and decreasing to 1.5–3 km s^{-1} at the map boundaries. The density of the emitting gas is greater than 10^4 cm^{-3} and the column density exceeds 10^{21} cm^{-2}. The correlation of the bright, narrow CO(7 → 6) lines with 158 μm [C II] emission suggests that over the entire region mapped, the narrow CO lines arise in warm photodissociation regions excited by ultraviolet (UV) photons from the Trapezium cluster. Although the Trapezium stars lie in front of the Orion A molecular cloud, not all of the warm gas is at the cloud surface. To the east of θ^1C the CO(7 → 6) lines split into two velocity components (also seen in $J = 2 \rightarrow 1$ ^{13}CO emission) which persist over several arcminutes. Since only one of these components can be on the surface, the other must arise from a dense, UV-illuminated clump or filament within the molecular cloud. Comparison of the quiescent CO(7 → 6) emission to CO(7 → 6) observed in a cross map of the energetic Orion KL outflow shows that the luminosity of shock-excited CO(7 → 6) emission in Orion is only a few percent of the luminosity of the widespread quiescent CO(7 → 6) emission.

Subject headings: ISM: individual (Orion Nebula) — ISM: kinematics and dynamics — ISM: molecules

1. INTRODUCTION

Recent observations of galactic star-forming regions indicate that ultraviolet (UV) photons from nearby or embedded OB stars can penetrate dense molecular cloud cores over parsec and greater scales, even though the interior regions appear well shielded from external UV radiation by large average dust column densities. UV photons with energies greater than 11.3 eV ionize atomic carbon, which radiates far-IR line emission at 158 μm. The bulk of the 158 μm [C II] emission arises in interface zones, or photodissociation regions (PDRs), on the surfaces of dense molecular regions ($n_{H_2} \gtrsim 10^3$ cm^{-3}) illuminated by the O or B stars (Crawford et al. 1985; Stacey et al. 1985; Wolfire, Hollenbach, & Tielens 1989). Maps of the far-IR 158 μm C^+ fine-structure line in M17, W3, and NGC 1977 show that the [C II] emission extends more than a parsec into dense molecular gas (Harris et al. 1987; Stutzki et al. 1988, Matsuhara et al. 1989; Howe et al. 1991), although in uniform dense gas the dust should attenuate the UV within a few hundredths of a parsec. Modeling of the intensity and distribution of the [C II] emission in M17, W3, and NGC 1977 shows that UV photons penetrate through a relatively transparent interclump medium, illuminate the surfaces of dense clumps or filaments, and produce the extended [C II] emission within the molecular clouds (Stutzki et al. 1988; Howe et al. 1991) rather than only near the UV sources.

In a PDR, a warm molecular layer with temperatures of up to several hundred degrees underlies the predominantly atomic region where most of the [C II] emission arises. Emission from rotational transitions of CO is an important coolant of the molecular component of a PDR (Tielens & Hollenbach 1985a; Sternberg & Dalgarno 1989) and dominates the gas cooling when the density is $\lesssim 10^5$ cm^{-3} (Sternberg & Dalgarno 1989). Most of the CO line luminosity is emitted by transitions from rotational states with energies from 120 to 300 K ($J = 6$ to 10) above the ground state (Burton, Hollenbach, & Tielens 1990). The CO(7 → 6) line is therefore a good tracer of the warm molecular component of a PDR. The small dipole moment of the CO molecule (0.11 debye) and its large abundance in molecular clouds ($[CO]/[H_2] \sim 10^{-4}$) make the rotational lines easily excited and relatively bright over a wide range of molecular gas temperatures and densities and make it possible to use these lines to derive the physical characteristics of the molecular gas.

The extensive distribution of PDRs in the M17, W3, and NGC 1977 molecular clouds suggests that widespread CO(7 → 6) emission, like [C II], may be common in high-mass star-forming regions. The Orion A region is a natural choice for a study of the extended spatial distribution of high-excitation molecular gas in a star-forming cloud. It is relatively nearby (distance ~470 pc; Genzel et al. 1981), giving a linear scale of 0.14 pc arcmin^{-1}, and bright submillimeter CO lines have been observed from quiescent gas and from the energetic compact outflow at Orion KL. Nearly all of the previous observations of the CO $J = 7 \rightarrow 6$ and $J = 6 \rightarrow 5$ emission lines in Orion have been confined to the inner few arcminutes centered on the Orion KL nebula (Fetterman et al. 1981; Goldsmith et al. 1981; Buhl et al. 1982; Koepf et al. 1982; Schultz et al. 1985; Graf et al. 1990). Schmid-Burgk et al. (1989) mapped the CO(7 → 6) emission from a 6′ × 8′ region encompassing Orion KL and the Trapezium OB cluster, Schmid-Burgk et al. (1989) mapped the CO(7 → 6) emission from a 6′ × 8′ region encompassing Orion KL and the Trapezium OB cluster, yielding good information about the core region. However, the moderate chopper throw (~2′) employed in the

[1] Department of Astronomy, University of Texas at Austin, Austin, TX 78712.
[2] Current address: Department of Astronomy, University of Maryland, College Park, MD 20742.
[3] Current address: National Institute of Standards and Technology, Division 814.03, 325 Broadway, Boulder, CO 80303.
[4] Current address: NASA/Goddard Space Flight Center, Code 685, Greenbelt, MD 20771.
[5] Department of Astronomy, Cornell University, Ithaca, NY 14853.

observations precluded a sensitive investigation of the large-scale CO(7 → 6) distribution.

We present here the results of a search for extended CO(7 → 6) line emission in the Orion A molecular cloud using the University of Texas submillimeter laser heterodyne receiver. We mapped the large-scale distribution of quiescent CO(7 → 6) emission along a cut across the Trapezium cluster extending more than 13′ (nearly 2 pc) in R.A. In contrast to the practice more common in high-frequency submillimeter heterodyne spectroscopy of spatially chopping with 2′–6′ throws, we employed the position-switching method where the telescope is slewed to a reference position well away from the source position to ensure against contamination from emission at the reference position. Our sensitivity to extended low-level line emission is limited, therefore, only by the receiver noise and the opacity of the atmosphere. We describe in § 2 the receiver, observing method, and calibration techniques. The CO(7 → 6) spectra and maps are presented in § 3. The physical parameters and energetics of the molecular gas are discussed in § 4. In § 5 we summarize the results of the investigation and compare our findings with observations of other high-luminosity star-forming regions.

2. OBSERVATIONS

We observed the $J = 7 \rightarrow 6$ rotational transition of CO ($\nu = 806.6517$ GHz, $\lambda = 371.6504$ μm) using the University of Texas submillimeter laser heterodyne receiver mounted at the Cassegrain focus of the 10.4 m telescope of the Caltech Submillimeter Observatory[6] (CSO) on 1990 December 2. The receiver employs a liquid-nitrogen cooled Schottky diode mounted in an open-structure 90° corner-reflecting mixer block (e.g., Kräutle, Sauter, & Schultz 1977). The local oscillator is an optically pumped submillimeter molecular laser operated at 802.986 GHz, which gives a first-intermediate frequency of 3.67 GHz. This signal is further mixed down to 1 GHz before sampling by the CSO backend 500 MHz acousto-optical spectrometer (AOS).

The receiver noise temperature measured on the telescope was 3850 K (double-sideband), and the measured zenith atmospheric transmission at 807 GHz was 0.32 (after correcting for the unequal atmospheric transmission at the signal and image sideband frequencies). The total scatter in the zenith transmission measured during the observations was less than ± 0.02. The absolute intensity scale was calibrated by observing blackbody loads at ambient and liquid-nitrogen temperatures placed in the signal beam path. We calibrated at each position observed, or every 5 minutes when we integrated at a single position for longer durations. The atmospheric transmission along the line of sight to the source was measured during each calibration series from the broad-band signal received from the sky. The observations were taken in position-switching mode with the reference position 30′ west of the mapping center position (θ^1C Orionis or Orion KL). Only first-order baseline corrections were applied to the spectra presented here, since both the atmosphere and the receiver were stable during the observations. The absolute pointing was established by maximizing the continuum signal received from a planet (Mars or Jupiter). We estimate that the absolute pointing accuracy is $\pm 7''$, with the relative pointing in the mapping observations accurate to $\pm 2''$ or less.

[6] The CSO is operated by the California Institute of Technology under funding from the National Science Foundation, contract AST 90-15755.

The telescope beam efficiency was measured using the continuum signals from Jupiter [diameter $D = (41'' \times 39'')^{1/2} = 40''$] and Mars ($D = 18''$), which was near opposition. Using a 372 μm brightness temperature of 143 K for Jupiter (Hildebrand et al. 1985, corrected for Jovian atmospheric absorption bands of HCN and PH_3 in the signal and image sidebands [Lellouch, Encrenaz, & Combes 1984]) and 220 K for Mars at opposition (Wright 1976; Wright & Odenwald 1980), we derive a coupling efficiency to Jupiter $\eta_{\rm Jup} = 0.24$, and a coupling efficiency to Mars $\eta_{\rm Mars} = 0.09$. The beam shape was determined from Gaussian profiles fitted to cross maps of Jupiter and Mars. The mapping data for both planets are well modeled by a beam that is the superposition of two Gaussian beams: a main beam of full width at half-maximum amplitude FWHM = 20″ and a broader error beam of FWHM = 90″, with an amplitude ratio of the main beam to the error beam of 9.4 to 1. These beam parameters also simultaneously reproduce the measured efficiencies on Jupiter and Mars, and give a total beam efficiency (the efficiency measured on a source that uniformly fills the sum of the two beam components) $\eta_{\rm tot} = 0.61$, which compares well with coupling efficiencies to the Moon measured on earlier observing runs, $\eta_{\rm Moon} = 0.65$. The coupling efficiency of this beam to Gaussian sources with FWHM = 30″, 60″, and 90″ is 0.18, 0.30, and 0.40, respectively. The effective solid angle subtended by the beam is $\Omega_{\rm beam} = 3.04 \times 10^{-8}$ sr, equivalent to the solid angle of a single 34″ FWHM Gaussian beam.

We also observed the $J = 2 \rightarrow 1$ transition of ^{13}CO ($\nu = 220.3987$ GHz, $\lambda = 1.3602$ mm) with the CSO facility 1.3 mm SIS receiver, also in position-switching mode, with the reference position 36′ north of the source (a position previously determined to be free of low-J CO emission). We used the standard chopper-wheel calibration method (Penzias & Burrus 1973) to correct for atmospheric attenuation and to set the thermal scale. The receiver noise temperature was ~420 K (single-sideband) and the atmospheric transmission was 0.92 or higher. The beam at 220 GHz is a single Gaussian with FWHM = 33″ ($\Omega_{\rm beam} = 2.86 \times 10^{-8}$ sr) and a main beam efficiency $\eta_{\rm MB} = 0.72$.

For the submillimeter observations we used the 1024-channel 500 MHz AOS, which gave a velocity resolution of 0.37 km s^{-1} and a total velocity coverage of 186 km s^{-1}. For the millimeter observations we used the 1024-channel 50 MHz AOS and the 500 MHz AOS, which gave velocity resolutions of 0.13 km s^{-1} and 1.34 km s^{-1} and total velocity coverages of 68 km s^{-1} and 680 km s^{-1}, respectively. We checked the frequency calibration and spectral resolution of the backend AOSs throughout the millimeter and submillimeter observations.

3. RESULTS

We observed bright, narrow CO(7 → 6) lines (velocity width $\Delta V \sim 1.5$–7.0 km s^{-1}) along a right ascension cut at the declination of θ^1C Ori (R.A.[1950] = 05^{h}32^{m}49^s, decl.[1950] = −05°25′16″) extending from 300″ west to 525″ east of θ^1C. The CO(7 → 6) spectra are shown in Figure 1. We also show in Figure 1 ^{13}CO(2 → 1) spectra observed at the same positions for comparison. The horizontal scale of each spectrum extends from $V_{\rm LSR} = -5$ to +25 km s^{-1}. The vertical scale gives the Rayleigh-Jeans antenna temperature of the CO(7 → 6) emission corrected for telescope losses and atmospheric attenuation (T_A^* in the notation of Kutner & Ulich 1981) divided by a 807 GHz beam coupling efficiency factor of 0.4. The beam coupling

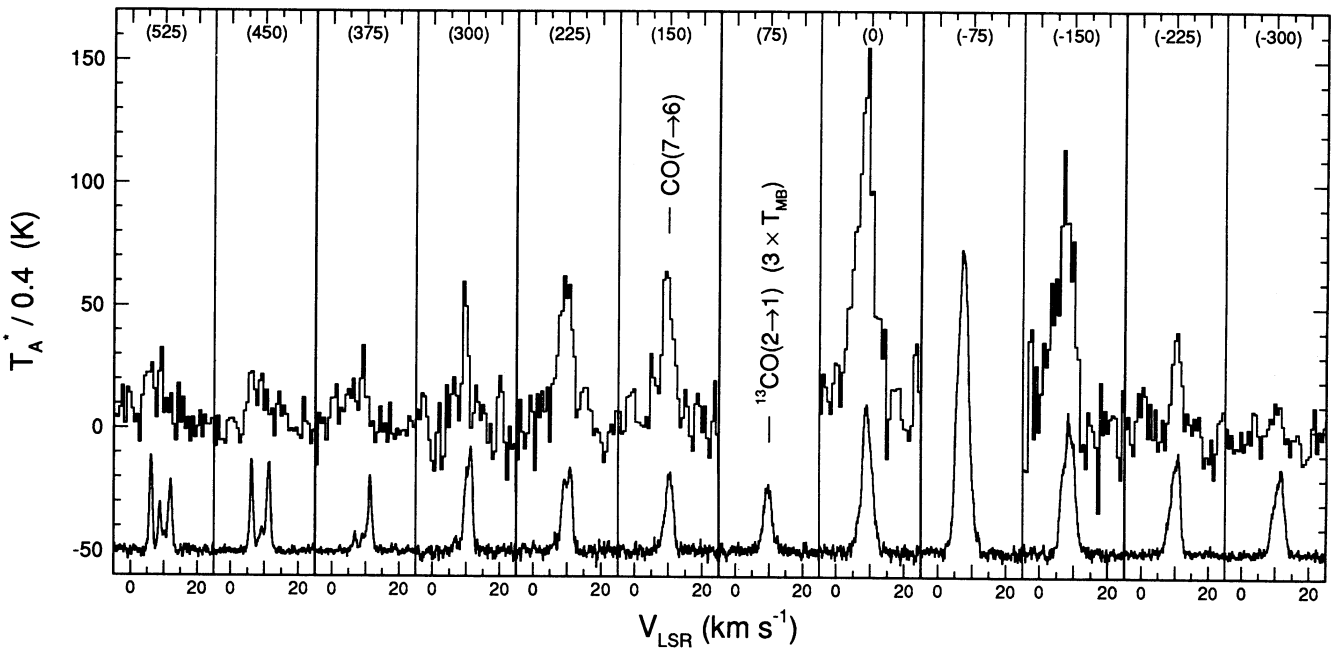

FIG. 1.—CO(7 → 6) (upper spectra) and ^{13}CO(2 → 1) (lower spectra) emission lines observed along a cut in R.A. in Orion. The 0″ position is at θ^1C Ori (R.A.[1950] = 05^{h}32^{m}49^s, decl.[1950] = −05°25′16″). The spacing between adjacent boxes is 75″, and the R.A. offset from θ^1C in arcseconds is given at the top of each box. The horizontal scale of each spectrum extends from $V_{LSR} = -5$ to +25 km s^{-1}. The vertical scale gives the Rayleigh-Jeans antenna temperature T_A^* of the CO(7 → 6) spectra divided by a 807 GHz beam coupling factor of 0.4. The ^{13}CO(2 → 1) spectra are plotted in units of 3 × T_{MB}.

factor is appropriate for sources such as Orion with brightness distributions which vary on moderately extended (∼90″) scales and is a good compromise between the coupling factors of very large uniform sources ($\eta_{tot} \sim 0.6$) and sources smaller than 60″ ($\eta \sim 0.3$). The ^{13}CO(2 → 1) spectra are plotted in units of Rayleigh-Jeans main beam brightness temperature T_{MB}, multiplied by a factor of 3 to facilitate comparison with the $J = 7 \rightarrow 6$ spectra. The spacing between the observed positions is 75″, except that time constraints prevented us from observing the CO(7 → 6) spectrum at the positions 75″ east and 75″ west of θ^1C. The CO(7 → 6) intensity map of Schmid-Burgk et al. (1989) indicates that the position of maximum peak line temperature, which we estimate is at least a factor of 1.15 higher than the line temperature toward θ^1C, is ∼40″ west of θ^1C. Our own ^{13}CO(2 → 1) observations also suggest that the CO(7 → 6) line temperature peaks at that position.

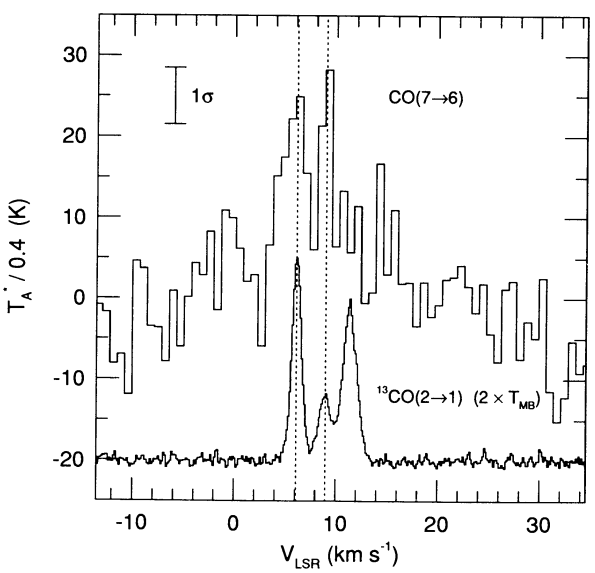

FIG. 2.—CO(7 → 6) and ^{13}CO(2 → 1) synthesized spectra generated by the co-addition of positions 450″ and 525″ east of θ^1C Ori. The vertical temperature scale gives T_A^* divided by 0.4 for the CO(7 → 6) spectrum and 2 × T_{MB} for the ^{13}CO(2 → 1) spectrum. The dotted lines mark the center velocity of the 6 and 9 km s^{-1} ^{13}CO line components. The 1 σ noise per channel for the CO(7 → 6) spectrum is also indicated.

The CO(7 → 6) lines are brightest within a few arcminutes of the Trapezium, with intensities ranging from 60 to 140 K and requiring molecular gas temperatures of at least 160 K near the exciting stars, substantially higher than the 55–85 K color temperature of the far-IR dust emission from the same region (Werner et al. 1976; Jaffe et al. 1984). To the west of θ^1C the line temperature drops from ∼40 K at 225″ west to ∼10 K at 300″ west, implying minimum kinetic temperatures of 57 K and 25 K, respectively. The CO(7 → 6) line intensity is ∼140 K at θ^1C and exceeds 50 K 300″ (0.7 pc) to the east. Emission is still detected 525″ (1.2 pc) east and 300″ west of θ^1C, with line temperatures of ∼25 K and ∼10 K, respectively, and most likely extends farther in both directions. The line widths also decrease with distance from θ^1C. At θ^1C the linewidth is ∼7 km s^{-1}, while 150″ and 225″ to the east the linewidth is ∼5 km s^{-1}. At 300″ east of θ^1C the linewidth has narrowed to only 1.8 km s^{-1}.

The velocity structure of both the CO(7 → 6) and the ^{13}CO(2 → 1) spectra becomes increasingly complex east of θ^1C, exhibiting multiple velocity components whose brightness vary from position to position. At positions beyond 375″ east of θ^1C, the CO(7 → 6) line profiles break up into two velocity components with narrow velocity widths ($\Delta V \sim 1.5$–2.0 km s^{-1}) and line temperatures of 25–30 K (implying minimum gas temperatures of 41–47 K). Figure 2 compares the ^{13}CO(2 → 1) and CO(7 → 6) line profiles for a spectrum synthesized by co-adding spectra at 450″ east and 525″ east of θ^1C to increase the

signal-to-noise ratio of the CO(7 → 6) spectrum. The CO(7 → 6) profile has velocity components at 6 and 9 km s^{-1} with line temperatures ~25 K. The ^{13}CO(2 → 1) spectrum also has components at 6 and 9 km s^{-1}, but with line temperatures differing by factor of ~3 (T_{MB} = 12 K and 4 K, respectively). In addition, there is a bright (T_{MB} = 10 K) ^{13}CO(2 → 1) component at 11 km s^{-1} with no observed counterpart in CO(7 → 6). More complete observations of the ^{13}CO emission sampled every 15″ in R.A. from 300″ east to 885″ east of θ^1C show that the velocity components persist on spatial scales of ~60″–120″.

In the following section we discuss the physical conditions and morphology of the emitting gas implied by the observations and the excitation of the submillimeter CO lines.

4. DISCUSSION

4.1. *Emission from Quiescent Gas*

4.1.1. *Gas Excitation near Ori θ^1C*

The local CO(7 → 6) intensity maximum near θ^1C indicates that the UV photons from the Trapezium stars are the excitation source for the CO(7 → 6) emission. The intense flux of Lyman continuum photons, contributed primarily by the O6 star θ^1C, dissociates and ionizes gas at the surface of the background Orion A cloud, creating an H II region ~5′ in diameter (Zuckerman 1973; Balick, Gammon, & Hjellming 1974). Between the H II region and the bulk of the molecular cloud lies a photodissociation region of partially ionized atomic and neutral molecular gas where the energetics are dominated by UV photons with energies less than the Lyman limit. Behind θ^1C, where the local UV flux G is roughly $10^5 G_0$ at the cloud surface ($G_0 = 1.6 \times 10^{-3}$ ergs s^{-1} cm^{-2}, the average interstellar flux of UV photons with energies of 6–13.6 eV), a PDR model well explains the observed far-IR [O I], [C I], and [C II] intensities (Tielens & Hollenbach 1985a, b). The observational result that the brightness temperature of the CO(7 → 6) line near θ^1C is more than twice the dust temperature in the same region, a condition observed only in molecular clouds with nearby UV sources, clearly rules out collisions with warm dust as the heating mechanism for the warm CO. In a PDR, however, the high flux of UV photons can directly heat the gas to temperatures higher than the dust component through collisions with electrons photoejected from dust grains and by collisional deexcitation of vibrationally excited, UV-pumped H_2. The similar morphology of the CO(7 → 6) emission (Schmid-Burgk et al. 1989) and the 158 μm [C II] emission (Stacey et al. 1993) in Orion strongly suggests a common origin for the excitation of these lines (Genzel & Stutzki 1989; Stacey et al. 1993). The narrow width of the CO(7 → 6) lines also makes it unlikely that shocks are important in heating the gas near the Trapezium stars.

4.1.2. *Temperature, Density, and Column Density Estimates*

We can use the observed CO(7 → 6) and ^{13}CO(2 → 1) line intensities and intensity ratios to estimate the temperature, density, and column density of the molecular gas. For gas densities of more than a few 10^3 cm^{-3} and temperatures higher than ~40 K, the intensity of the CO(7 → 6) line emission depends more sensitively on the physical conditions in the emitting gas than do the millimeter CO transitions (the J = 7 rotational level lies 155 K above the ground state and the critical density of the J = 7 → 6 transition is $n_{crit} \sim 6 \times 10^5$ cm^{-3}). Although there is ample evidence that the molecular gas in Orion is far from uniform, we assume for the moment that the CO and ^{13}CO lines are emitted from a uniform gas at a single temperature and density (§ 4.1.4 outlines some of the effects of relaxing this assumption). The uniform model results set lower limits to the actual temperature, density, and column density of the PDR layers, as we discuss later. We adopt a value of 60 for the [^{12}CO]/[^{13}CO] abundance ratio in Orion (see Blake et al. [1987] for a discussion of abundances in Orion). We compare the observed line intensities and ratios with line intensities computed from a non–LTE large velocity gradient (LVG) radiative transfer model (Scoville & Solomon 1974; Goldreich & Kwan 1974) to estimate the range of the physical conditions of the emitting gas. An LVG model is the simplest way to include non–LTE effects and local radiative trapping in the estimation of the physical conditions from the line intensities. The model employs the H_2–CO collision rate constants of Schinke et al. (1985) and Flower & Launay (1985) and assumes a plane-parallel cloud geometry. Figure 3 shows the LVG model result for a ^{12}CO column density per unit velocity interval $N_{CO}/dV = 10^{18}$ cm^{-2} km^{-1} s. The model results indicate that uniform gas with temperatures of 40–200 K, molecular hydrogen densities n_{H_2} of 10^3–10^5 cm^{-3}, and CO column densities N_{CO} of 2×10^{17}–4×10^{18} cm^{-2} can reproduce the entire observed range of detected CO(7 → 6) line intensities (25 K < $T_A^*/(0.4)$ < 140 K) and CO(7 → 6) to ^{13}CO(2 → 1) intensity ratios (which range from 2 to 15). For example, at the position 150″ west of θ^1C, $N_{CO} \sim 2 \times 10^{18}$ cm^{-2}, $n_{H_2} > 6 \times 10^4$ cm^{-3}, and $T_{gas} \sim 110$ K produces the observed line intensity of 98 K and CO(7 → 6) to ^{13}CO(2 → 1) ratio, while at the position 450″ east of θ^1C, the best LVG

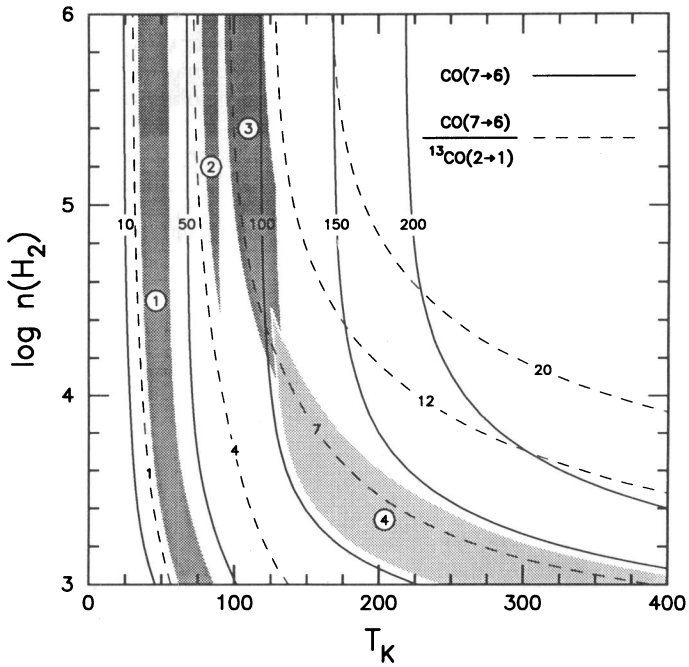

FIG. 3.—The LVG model for a ^{12}CO column density per unit velocity interval $N_{CO}/dV = 10^{18}$ cm^{-2} km^{-1} s, plotted in the temperature-density plane. Solid contours give the Rayleigh-Jeans brightness temperature of the J = 7 → 6 transition of CO, while the dashed contours denote the brightness temperature ratio of CO(7 → 6) to ^{13}CO(2 → 1). The gray regions 1, 2, 3, and 4 show the intersection of the value of CO(7 → 6) $T_A^*/0.4$ (±1 σ) with the CO(7 → 6) $T_A^*/0.4$ to ^{13}CO(2 → 1) T_{MB} ratio (±1 σ) for positions (525, 0), (150, 0), (−150, 0), and (0, 0), respectively.

model fit for the 9 km s^{-1} velocity component is obtained with $N_{CO} \sim 2 \times 10^{17}$ cm^{-2} and n_{H_2} varying from 10^3 to $10^{4.5}$ cm^{-3} as T_{gas} goes from 200 to 50 K. At a few positions, any density $n_{H_2} > 10^4$ cm^{-3} gives an acceptable line intensity for one combination of temperature and column density within the range of temperatures and column densities given above. For the bright ^{13}CO(2 → 1) velocity components ($T_{MB} > 10$ K) which have no observable counterpart in CO(7 → 6), such as the 11 km s^{-1} component at positions farther than 150″ east of θ^1C, CO column densities of about 10^{18} cm^{-2} and low temperatures (less than 40 K) are required for excitation conditions that produce the observed ^{13}CO line temperatures without simultaneously increasing the CO(7 → 6) line temperature to an observable level.

4.1.3. *Excitation of Extended Emission*

The large-scale distribution of [C II] emission, especially east of θ^1C, is similar to the distribution of CO(7 → 6) emission (Fig. 4) and suggests that the [C II] and CO lines share a common PDR origin across the *entire* region mapped and not only in the immediate vicinity of the Trapezium. Mapping of the 158 μm [C II] line across the Trapezium region shows that the [C II] line arises from a region more than 30′ (4 pc) in extent (Stacey et al. 1993), and indicates the presence of a large UV flux (higher than 100 G_0) beyond the limits of our CO(7 → 6) observations. A more detailed fully-sampled map of the [C II] emission in the inner few arcminutes around θ^1C shows that the [C II] emission peaks just west of the Trapezium (Stacey et al. 1993), as does the CO(7 → 6) emission. The steep decline in [C II] emission to the west of θ^1C, in the same region where the CO(7 → 6) emission is at a maximum, is a consequence of the high density of the gas ($n_{H_2} > 10^5$ cm^{-3}) west of the Trapezium traced by clumps of CS(2 → 1) emission (Mundy et al. 1986, 1988). At densities $\gtrsim 10^5$ cm^{-3}, the self-shielding of the CO from dissociating UV radiation raises the column density of warm CO in the PDR relative to the column density of C^+ and increases the relative strength of the CO emission to the [C II] emission (Wolfire et al. 1989).

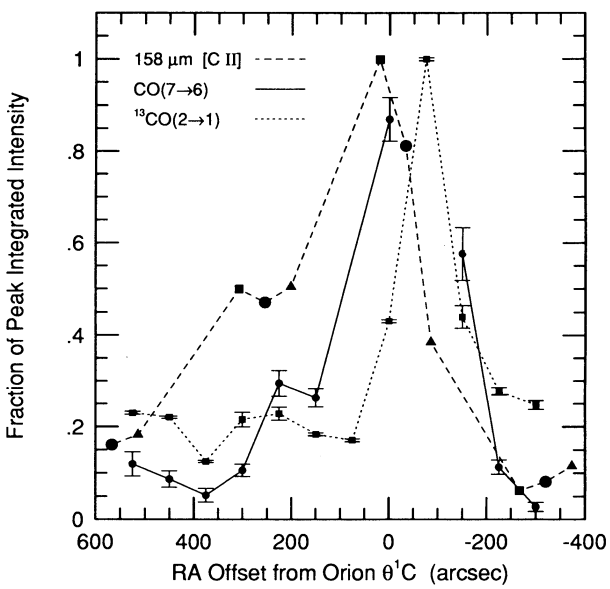

FIG. 4.—Comparison of the integrated intensity over all velocity components of the CO(7 → 6), ^{13}CO(2 → 1), and 158 μm [C II] emission along the θ^1C Ori cut. The peak intensities are 6.1 × 10^{-4}, 1.8 × 10^{-6}, and 4.2 × 10^{-3}, respectively, in units of ergs s^{-1} cm^{-2} sr^{-1}. The [C II] data are from Stacey et al. (1993). The peak intensity of the CO(7 → 6) emission along the R.A. cut is estimated from an extrapolation based on the map of Schmid-Burgk et al. (1989). The CO(7 → 6) peak lies between positions 0″ and −150″.

The CO(7 → 6) emission in the region ∼1 pc east of θ^1C probably also arises in PDRs, since the [C II] emission from that region indicates the presence of a PDR there (Stacey et al. 1993). The flux of UV photons from the Trapezium stars in this region is at least 100 G_0, based on the observed [C II] line intensity, and could be as much as a few 10^3 G_0. The UV flux 1 pc east of θ^1C is similar to the UV flux in the reflection nebula NGC 2023, where bright CO(7 → 6) lines ($T_{MB} \sim 70$ K) are emitted from a PDR (Jaffe et al. 1990). Thus, a PDR origin for the quiescent ($\Delta V < 2$ km s^{-1}) extended CO(7 → 6) emission in Orion, even in regions of moderate UV photon flux (100–1000 G_0), is not without precedent.

4.1.4. *Evidence for Emission from Clump Surfaces*

The coexistence of the 6 and 9 km s^{-1} CO(7 → 6) velocity components over arcminute length scales makes it unlikely that both components are at the surface of the molecular cloud; more likely the components are emitted by spatially distinct clumps or filaments separated along the line of sight and illuminated by the UV flux from the Trapezium. Observations and models of M17 (Harris et al. 1987; Stutzki et al. 1988), and W3 and NGC 1977 (Howe et al. 1991), demonstrate that PDR emission from the surfaces of dense clumps or filaments can extend over parsec length scales through molecular clouds. Furthermore, Tauber & Goldsmith (1990) find that the CO and ^{13}CO $J = 3 \rightarrow 2$ intensities and line profiles in Orion are poorly fitted by models with uniform gas, but are better explained by a model composed of spherical clumps with radial temperature and density gradients illuminated by an external UV field. On size scales of a parsec or more, the ^{13}CO(1 → 0) map by Bally et al. (1987) shows that the Orion A cloud is composed of a highly nonuniform complex of filaments and clumps. Ziurys et al. (1981) and Batrla et al. (1983) observed in the (1, 1) and (2, 2) inversion lines of NH_3 a series of clumps in the Orion ridge with ∼0.1 pc diameters and smaller. At still smaller scales, interferometric maps of the emission from the $J = 2 \rightarrow 1$ transition of CS at 7″.5 resolution reveal four distinct clumps ∼30″ west of the Trapezium with diameters ranging from 15″ to 50″ (0.04–0.12 pc) and densities greater than 10^5 cm^{-3} (Mundy et al. 1986, 1988). Our own ^{13}CO(2 → 1) and CO(7 → 6) observations reveal multiple velocity components persisting over ∼1′ length scales and with varying excitation conditions, particularly in the region a parsec or more east of θ^1C. Observations of the C109α carbon recombination line in Orion A at a spatial resolution of 2′.6 show two velocity components ($V_{LSR} \sim 6$ and 10–11 km s^{-1}) at positions 170″ east and 327″ east of θ^1C (Jaffe & Pankonin 1978). A spectrum of the 158 μm [C II] line 4′ east of θ^1C at 0.8 km s^{-1} spectral resolution also shows two components, at $V_{LSR} \sim 6$ and 11 km s^{-1} (Boreiko, Betz, & Zmuidzinas 1988).

The temperature, density, and column density of the molecular gas must be higher in a nonuniform, clumpy medium than the results of the uniform, single temperature and density models suggest. In a clumped gas, the beam area filling factor can decrease from its value for a smoothly varying gas. The observed peak brightness temperatures of the CO(7 → 6) lines could then underestimate the true excitation temperature of the gas and imply kinetic temperatures higher than the 40 K brightness temperatures of the region ∼1 pc east of θ^1C. The

local CO column densities within the clumps must also increase to preserve the average value sampled within a beam diameter. The higher gas temperatures implied by a clumped gas decrease the fractional abundance of ^{13}CO molecules in the $J = 2$ state by populating higher energy states, increasing further the local CO column density required by the observed $^{13}CO(2 \rightarrow 1)$ line intensities. The density of the gas in the clumps must then increase so that the larger CO column densities do not require excessively large clump diameters. In a clumped or filamentary gas, then, the $CO(7 \rightarrow 6)$ and $^{13}CO(2 \rightarrow 1)$ observations require the results of the simple LVG models to be interpreted strictly as lower limits to the actual temperatures, densities, and column densities of the emitting regions. Indeed, the observed integrated intensities of the extended component of the $CO(7 \rightarrow 6)$ emission lines imply densities $\gtrsim 10^5$ cm^{-3} if the lines arise in PDRs (Burton, Hollenbach, & Tielens 1990). Even if the CO is heated by collisions with warm dust, a gas density greater than 10^5 cm^{-3} is required for the collisional heating rate to equal the luminosity of the CO emission.

Although the evidence supports the contention that the $CO(7 \rightarrow 6)$ lines a parsec east of θ^1C arise in PDRs on the surface of embedded clumps or filaments, a definitive answer as to the excitation mechanism requires further observations. The color temperature of the far-IR dust continuum emission from that region, as derived from *IRAS* data, ranges from ~ 35 K to 65 K, depending on the power of the dust emissivity ($1 \leq \beta \leq 2$, where we assume the dust emissivity varies with wavelength as $\lambda^{-\beta}$). Since the brightness of the $CO(7 \rightarrow 6)$ lines in the same region requires gas temperatures of at least 40 K, we can say only that $T_{\rm gas} \approx T_{\rm dust}$, leaving open the possibility that the gas is heated by collisions with the dust. Observations such as the high-resolution maps of CS emission (Mundy et al. 1986, 1988), however, support a clumpy morphology to the gas, in which case the gas temperature could be considerably higher than the lower limit derived here. If the gas is indeed clumped on scales smaller than the 807 GHz beam, observations at higher spatial resolution should detect $CO(7 \rightarrow 6)$ line temperatures higher than the 25 K brightness temperatures we observe. Observations of the 158 μm [C II] line in this region at a spectral resolution sufficient to resolve the velocity components seen in the $CO(7 \rightarrow 6)$ and $^{13}CO(2 \rightarrow 1)$ lines could determine if the velocity and width of the [C II] line emission are the same as one, both, or neither of the $CO(7 \rightarrow 6)$ velocity components and would indicate a PDR origin of the emission if the $CO(7 \rightarrow 6)$ and [C II] line widths and velocities were the same. The lack of a $CO(7 \rightarrow 6)$ line component at the $+11$ km s^{-1} velocity of one of the C109α and [C II] line components may indicate a low density ($n \sim 10^3$ cm^{-3}) for the gas emitting those lines, and therefore a very subthermal population of CO in the $J = 7$ state. Observations of spectrally resolved 158 μm [C II] lines at the velocities of the $CO(7 \rightarrow 6)$ line components and observations at higher spatial resolution of $CO(7 \rightarrow 6)$ brightness temperatures higher that the dust temperature in the same region would conclusively demonstrate the PDR origin of the emission, rather than heating by shocks or by collisions with warm dust.

4.2. *Emission from Shocked Gas: Orion KL*

About 1′ north of θ^1C lies the energetic outflow source, Orion KL. In marked contrast to the narrow velocity width and wide spatial extent of the quiescent PDR emission excited by the Trapezium cluster, the Orion KL region exhibits extremely energetic mass motions [$\Delta V \sim 100$ km s^{-1} full width to zero power (FWZP) in the $CO(7 \rightarrow 6)$ emission lines] confined to a region less than 1′ in extent. Figure 5 shows the $CO(7 \rightarrow 6)$ spectra observed toward Orion KL. The cross map is centered at R.A.(1950) = $05^h32^m47^s.0$ and decl.(1950) = $-05°24'25''$, and the spacing between the observed positions is 10″ in R.A. and in decl. The horizontal scale of each spectrum extends from $V_{\rm LSR} = -80$ to $+100$ km s^{-1}. Linear baselines were removed from the spectra, which have been smoothed to a spectral resolution of ~ 1.5 km s^{-1} per channel. The vertical scale of each spectrum extends from -100 to $+500$ K in units of T_A^* divided by an efficiency factor of 0.20, which is appropriate for the coupling of the beam to a Gaussian source with FWHM $\sim 35''$. This size scale is relevant only to the wing emission and not to the line core, for which the temperature scale produces artificially high temperatures (by approximately a factor of 2).

The most striking aspect of the wing emission is its absolute brightness. At all positions within 10″ of the map center, the line temperature exceeds 200 K even for emission 20 km s^{-1} blueward of the line center velocity at 9 km s^{-1}, implying a kinetic temperature of at least 220 K. The line temperature of similarly redshifted emission at the same positions is about 100 K less than the blueshifted emission. Wing emission at velocities more than ± 20 km s^{-1} from the line center velocity traces the high-velocity flow seen in the millimeter CO transitions and is not likely affected by the hot, low-velocity flow seen in the 3 mm rotational transitions of SiO and SO (ΔV[FWZP] ~ 35 km s^{-1}; Genzel & Stutzki 1989). At 20″ south of KL, the wing emission has decreased enough so that the bright spike feature characteristic of extended ridge emission becomes readily apparent. Significant wing emission is still present 20″ north of KL, in agreement with the five-point $CO(7 \rightarrow 6)$ cross map of KL obtained at 45″ spacing by Schmid-Burgk et al. (1989). The integrated intensity of the blue wing emission generally exceeds that of the red wing, a feature also seen in the 2.1 μm H_2 $v = 1 \rightarrow 0$ $S(1)$ line emission from hot shock-excited gas in the KL region (Nadeau & Geballe 1979), indicating that the excess blue emission in the H_2 line profiles may not be an artifact of higher extinction of the red wing emission. Excess blue wing emission is also seen in the line profiles of shock-excited 63 μm [O I] emission from the KL region (Werner et al. 1984). We note that although the line core emission appears to be weakest at the central position in the cross map, further observations are needed to confirm this result.

4.2.1. *Outflow Size and Morphology*

The wing emission is spatially compact and exhibits marked differences in both the absolute and relative intensities of the red and blueshifted wing emission at adjacent positions in the map. Although the high-velocity emission extends beyond the limits of the region mapped, particularly to the north and west, the extent of the emission to the half-power level is $\sim 40''$ in R.A. and $\sim 35''$ in decl. This extent implies a source size less than 35″ in R.A. by 28″ in decl. if the emission has a Gaussian distribution, consistent with 35″ resolution $CO(6 \rightarrow 5)$ mapping results (FWHM $\sim 45'' \times 35''$; Koepf et al. 1982). For a source of this size, roughly 75% of the received power is detected by the 20″ main beam. The $CO(7 \rightarrow 6)$ emission region

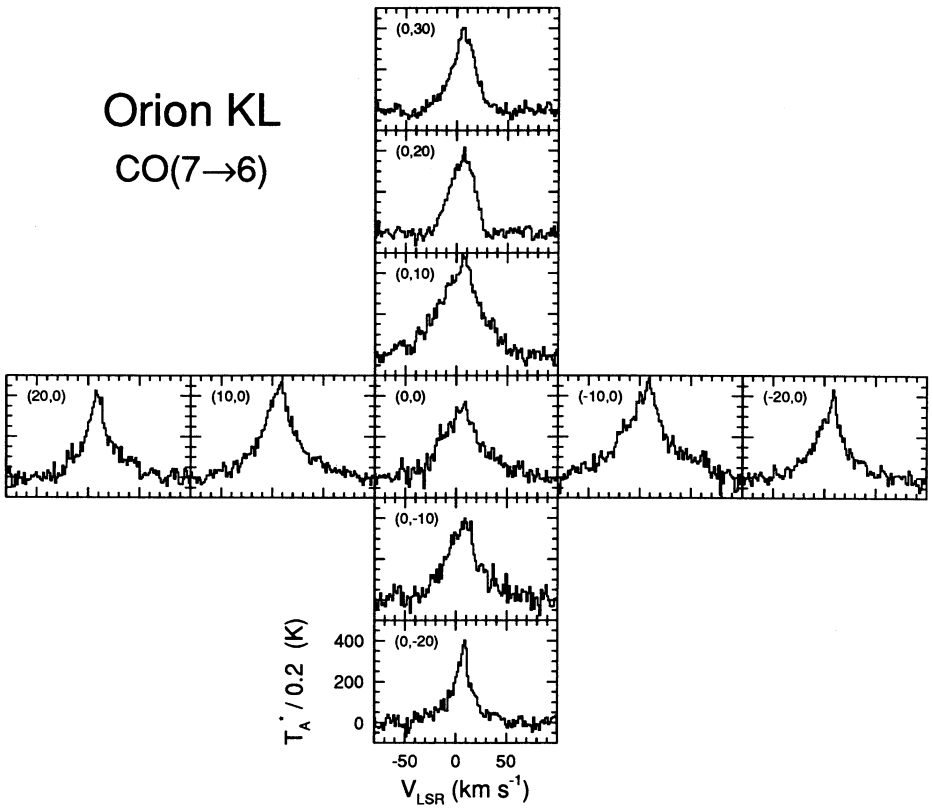

FIG. 5.—Cross map of CO(7 → 6) spectra observed toward Orion KL. The (0, 0) position is at R.A.(1950) = 05^{h}32^{m}47^s.0 and decl.(1950) = −05°24′25″, and the spacing between the observed positions is 10″ in R.A. and in decl. The horizontal scale of each spectrum extends from V_{LSR} = −80 to +100 km s^{-1}. The vertical scale of each spectrum extends from −100 to 500 K in units of T_A^* divided by a beam coupling factor of 0.2, which is appropriate for the wing emission but not for the line core. The R.A. and decl. offsets in arcseconds from the (0, 0) position are indicated in the upper left corner of each spectrum.

lies within the ∼75″ FWHM region emitting 2 μm H_2 rovibrational lines (Beckwith et al. 1978) and far-IR CO lines (Watson et al. 1985). Our data do not unambiguously indicate a bipolar structure to the outflow, so the separation of the centroids of the redshifted and the blueshifted emission distributions must be small. The morphology of the high-velocity flow traced by the CO(7 → 6) emission is consistent with the data of Erickson et al. (1982), which show that the extent of the redshifted and blueshifted CO(3 → 2) emission contours is ∼30″–40″ to the half-power level, that the centroids of the red and blue lobes of the outflowing gas are separated by ∼12″, and that the integrated intensity of the blue wing is greater than the integrated intensity of the red wing.

4.2.2. *Density and Column Density Estimates*

The CO(7 → 6) wing emission is probably emitted by cooling postshock gas downstream of the hot (∼2000 K) gas traced by 2 μm H_2 thermal rovibrational line emission (Beckwith et al. 1978; Beckwith, Persson, & Neugebauer 1979; Scoville et al. 1982; Beckwith et al. 1983). The bulk of the column density of the gas emitting the CO(7 → 6) line must be colder than the ∼750 K temperature characteristic of the gas emitting the far-IR CO lines detected by Watson et al. (1985), since the integrated intensity of the CO(7 → 6) wing emission is about an order of magnitude greater than can be emitted by the hotter component; molecular gas at a temperature of 750 K or higher with a sufficient column density to emit the observed CO(7 → 6) line intensity would also emit far-IR CO line emission much brighter than observed. The column density of the gas emitting the bulk of the CO(7 → 6) wing emission is at least 5×10^{22} cm^{-2} (where we use the non–LTE CO emission coefficients of McKee et al. 1982 and assume an excitation temperature of ∼250–500 K, density $n_{H_2} \sim 10^5$–10^6 cm^{-3}, and CO abundance of 10^{-4} relative to H_2), substantially greater than the column density of the gas emitting the far-IR CO lines (∼3×10^{21} cm^{-2}; Watson et al. 1985) or the IR H_2 lines (∼3×10^{19} cm^{-2}; Watson et al. 1985). We derive a lower limit to the density of the outflowing gas $n_{H_2} > 3 \times 10^5$ cm^{-3} from the lower limit to the column density and a 30″ source diameter. The small size of the CO(7 → 6) emission region compared with that of the region encompassing the hot gas emitting the H_2 IR rovibrational lines and the far-IR CO lines indicates that the submillimeter CO emission lines arise in gas closer to the outflow source and supports the contention that the gas is cooling downstream of the hot gas shocked by the outflow.

5. CONCLUSIONS

We observed CO(7 → 6) emission across a region nearly 2 pc in extent in the core of the Orion A cloud. Emission is observed out to the limits of the mapping and undoubtedly extends farther. The line temperature of the extended CO(7 → 6) emission out to more than 8′ from the peak position is still about

0.2 of the peak observed line temperature. Except at the position of Orion KL, the narrow line profiles ($\Delta V < 7$ km s^{-1}) indicate a relatively quiescent excitation mechanism. The line intensities constrain the gas to temperatures greater than 40 K across the entire region mapped. Comparison of the quiescent CO(7 → 6) line strengths with emission from ^{13}CO(2 → 1) indicates that the densities of the emitting gas must be greater than 10^4–10^5 cm^{-3} and the H_2 column densities must exceed 10^{21}–10^{22} cm^{-2} for this component.

There is good evidence that the submillimeter CO emission arises from PDRs excited by the far-UV flux from the Trapezium cluster. Bright 158 μm [C II] line emission, which is excited in the primarily atomic component of PDRs, radiates from the entire region mapped in the CO(7 → 6) line. The line strength of the quiescent CO(7 → 6) emission peaks near θ^1C and indicates a gas temperature higher than 160 K, more than twice the temperature of the dust at the same position and ruling out collisions with dust as a heating mechanism for the gas. In PDRs, however, UV can directly heat the gas to temperatures exceeding the dust temperature. The PDR models of Burton et al. (1990) can reproduce the observed integrated intensities of the quiescent CO(7 → 6) emission in the regions a parsec or more from θ^1C, where the UV flux is less than a few $10^3 G_0$, as long as $n_{H_2} \gtrsim 10^5$ cm^{-3}.

Perhaps the most interesting aspect of the CO(7 → 6) spectra is the emergence of multiple velocity components in the region 6′ east of θ^1C and beyond. Such a phenomenon is easily explained if the molecular gas is highly clumped, as a number of observations of the Orion A cloud indicate. We interpret the multiple components as emission from two distinct clumps or filaments separated along the line of sight, at least one of which must be embedded in the cloud. The presence of bright [C II] emission from the same region and observations of multiple C^+ velocity components in carbon radio recombination lines suggest that the CO(7 → 6) lines are emitted from PDRs on the clump or filament surfaces. Like the [C II] emission from the molecular clouds associated with M17, W3, and NGC 1977, the CO lines in Orion probably arise in PDRs throughout the interior of the molecular cloud and not only at the surface. Spectrally resolved observations of the 158 μm [C II] line will be needed to positively correlate the [C II] emission with one or both of the CO components.

Quiescent emission dominates the total flux of CO(7 → 6) line emission from Orion A. Although the brightest lines, with a total velocity extent of ~100 km s^{-1} and brightness temperatures exceeding 250 K, are emitted from the Orion KL region, the compactness of the outflow source diminishes the contribution of the broad-line emission to only a few percent of the total flux of CO(7 → 6) emission from Orion A. Generalizing the results of the distribution of CO(7 → 6) line flux along the cut in R.A. through θ^1C to two dimensions, we find that the emission from regions between 6′ and 9′ from θ^1C, where the UV flux is less than a few $10^3 G_0$, contributes ~0.3 of the total CO(7 → 6) line flux, while emission from the brightest quiescent lines within ~75″ of θ^1C account for only ~0.1 of the total line flux. The balance of the line flux arises in the region between 75″ and 6′ from θ^1C. Mapping of the CO(7 → 6) line in other molecular clouds with moderate ambient UV fields ($G \sim 100$–$1000\ G_0$) can determine whether widespread low-level emission ($T_B < 50$ K) dominates the total flux of CO(7 → 6) emission. A good candidate for such a mapping project is the Orion B molecular cloud, where the ambient UV field strength varies from ~40 to 500 G_0 and where bright 158 μm [C II] emission extends over most of a 24′ × 36′ region encompassing the H II region NGC 2024 and the reflection nebula NGC 2023 (Jaffe et al. 1993).

The Orion A cloud offers an interesting contrast to the more distant and more luminous star-forming regions DR 21 and W51, where broad-line CO(7 → 6) emission ($\Delta V > 20$ km s^{-1}) is observed to extend over 2–3 pc scales and dominates the total flux emanated in the $J = 7 \rightarrow 6$ transition (Jaffe et al. 1989). If the Orion cloud were at the same distance as DR 21 or W51 (~5 kpc), the broad-line CO(7 → 6) emission from Orion KL would be completely unobservable due to beam dilution, given the present sensitivity of 800 GHz receivers, and only the extended quiescent component would be detected.

We thank H. Dinerstein, N. Evans, D. Hollenbach, and J. Lacy for helpful critiques of early drafts of this work. The observations would not have been possible without the able technical support of the staff of the CSO. J. E. H. acknowledges support from a NASA Graduate Student Researchers Program fellowship. This research was supported by the University of Texas at Austin, NSF grant 88-17544, and a grant from the W. M. Keck Foundation.

REFERENCES

Balick, B., Gammon, R. H., & Hjellming, R. M. 1974, PASP, 86, 616
Bally, J., Langer, W. D., Stark, A. A., & Wilson, R. W. 1987, ApJ, 312, L45
Batrla, W., Wilson, T. L., Bastien, P., & Ruf, K. 1983, A&A, 128, 279
Beckwith, S., Evans, N. J., II, Gatley, I., Gull, G., & Russell, R. W. 1983, ApJ, 264, 152
Beckwith, S., Persson, S. E., & Neugebauer, G. 1979, ApJ, 227, 436
Beckwith, S., Persson, S. E., Neugebauer, G., & Becklin, E. E. 1978, ApJ, 223, 464
Blake, G. A., Sutton, E. C., Masson, C. R., & Phillips, T. G. 1987, ApJ, 315, 621
Boreiko, R. T., Betz, A. L., & Zmuidzinas, J. 1988, ApJ, 325, L47
Buhl, D., Chin, G., Koepf, G. A., Peck, D. D., & Fetterman, H. R. 1982, in Submillimetre Wave Astronomy, ed. J. E. Beckman & J. P. Phillips (Cambridge: Cambridge Univ. Press), 111
Burton, M. G., Hollenbach, D. J., & Tielens, A. G. G. M. 1990, ApJ, 365, 620
Crawford, M. K., Genzel, R., Townes, C. H., & Watson, D. M. 1985, ApJ, 291, 755
Erickson, N. R., Goldsmith, P. F., Snell, R. L., Berson, R. L., Huguenin, G. R., Ulich, B. L., & Lada, C. J. 1982, ApJ, 261, L103
Fetterman, H. R., et al. 1981, Science, 211, 580
Flower, D. R., & Launay, J. M. 1985, MNRAS, 214, 271
Genzel, R., Reid, M. J., Moran, J. M., & Downes, D. 1981, ApJ, 244, 884
Genzel, R., & Stutzki, J. 1989, ARA&A, 27, 41
Goldreich, P., & Kwan, J. 1974, ApJ, 189, 441
Goldsmith, P. F., et al. 1981, ApJ, 243, L79
Graf, U. U., Genzel, R., Harris, A. I., Hills, R. E., Russell, A. P. G., & Stutzki, J. 1990, ApJ, 358, L49
Harris, A. I., Stutzki, J., Genzel, R., Lugten, J. B., Stacey, G. J., & Jaffe, D. T. 1987, ApJ, 322, L49
Hildebrand, R. H., Loewenstein, R. F., Harper, D. A., Orton, G. S., Keene, J., & Whitcomb, S. E. 1985, Icarus, 64, 64
Howe, J. E., Jaffe, D. T., Genzel, R., & Stacey, G. J. 1991, ApJ, 373, 158
Jaffe, D. T., Davidson, J. A., Dragovan, M., & Hildebrand, R. H. 1984, ApJ, 284, 637
Jaffe, D. T., Genzel, R., Harris, A. I., Howe, J. E., Stacey, G. J., & Stutzki, J. 1990, ApJ, 353, 193
Jaffe, D. T., Genzel, R., Harris, A. I., Lugten, J. B., Stacey, G. J., & Stutzki, J. 1989, ApJ, 344, 265
Jaffe, D. T., & Pankonin, V. 1978, ApJ, 226, 869
Jaffe, D. T., et al. 1993, in preparation
Koepf, G. A., Buhl, D., Chin, G., Peck, D. D., Fetterman, H. R., Clifton, B. J., & Tannenwald, P. E. 1982, ApJ, 260, 584
Kräutle, H., Sauter, E., & Schultz, G. V. 1977, Infrared Phys., 17, 477
Kutner, M. L., & Ulich, B. L. 1981, ApJ, 250, 341
Lellouch, E., Encrenaz, T., & Combes, M. 1984, A&A, 140, 405
Matsuhara, H., et al. 1989, ApJ, 339, L67
McKee, C. F., Storey, J. W. V., Watson, D. M., & Green, S. 1982, ApJ, 259, 647
Mundy, L. G., Cornwell, T. J., Masson, C. R., Scoville, N. Z., Baath, L. B., & Johansson, L. E. B. 1988, ApJ, 325, 382

Mundy, L. G., Scoville, N. Z., Baath, L. B., Masson, C. R., & Woody, D. P. 1986, ApJ, 304, L51
Nadeau, D., & Geballe, T. R. 1979, ApJ, 230, L169
Penzias, A. A., & Burrus, C. A. 1973, ARA&A, 11, 51
Schinke, R., Engel, V., Buch, U., Meyer, H., & Diercksen, G. H. F. 1985, ApJ, 299, 939
Schmid-Burgk, J., et al. 1989, A&A, 215, 150
Schultz, G. V., Durwen, E. J., Röser, H. P., Sherwood, W. A., & Wattenbach, R. 1985, ApJ, 291, L59
Scoville, N. Z., Hall, D. N. B., Kleinmann, S. G., & Ridgway, S. T. 1982, ApJ, 253, 136
Scoville, N. Z., & Solomon, P. M. 1974, ApJ, 187, L67
Stacey, G. J., Jaffe, D. T., Geis, N., Genzel, R. Harris, A. I., Poglitsch, A., Stutzki, J., & Townes, C. H. 1993, ApJ, 404, 219
Stacey, G. J., Viscuso, P. J., Fuller, C. E., & Kurtz, N. T. 1985, ApJ, 289, 803
Sternberg, A., & Dalgarno, A. 1989, ApJ, 338, 197
Stutzki, J., Stacey, G. J., Genzel, R., Harris, A. I., Jaffe, D. T., & Lugten, J. B. 1988, ApJ, 332, 379
Tauber, J. A., & Goldsmith, P. F. 1990, ApJ, 356, L63
Tielens, A. G. G. M., & Hollenbach, D. 1985a, ApJ, 291, 722
———. 1985b, ApJ, 291, 747
van Dishoeck, E. F., & Black, J. H. 1988, ApJ, 334, 771
Watson, D. M., Genzel, R. Townes, C. H., & Storey, J. W. V. 1985, ApJ, 298, 316
Werner, M. W., Crawford, M. K., Genzel, R. Hollenbach, D. J., Townes, C. H., & Watson, D. M. 1984, ApJ, 282, L81
Werner, M. W., Gatley, I., Harper, D. A., Becklin, E. E., Loewenstein, R. F., Telesco, C. M., & Thronson, H. A. 1976, ApJ, 204, 420
Wolfire, M. G., Hollenbach, D., & Tielens, A. G. G. M. 1989, ApJ, 344, 770
Wright, E. L. 1976, ApJ, 210, 250
Wright, E. L., & Odenwald, S. 1980, BAAS, 12, 456
Ziurys, L. M., Martin, R. N., Pauls, T. A., & Wilson, T. L. 1981, A&A, 104, 288
Zuckerman, B. 1973, ApJ, 183, 163